Eur. Phys. J. B **3**, 237–245 (1998)

THE EUROPEAN PHYSICAL JOURNAL B

Field-induced winding of chiral polymers

P.I.C. Teixeira and E.M. Terentjev[a]

Cavendish Laboratory, Madingley Road, Cambridge CB3 0HE, UK

Received: 15 November 1997 / Accepted: 16 February 1998

Abstract. We propose a microscopic model of a chiral polymer chain with permanent transverse dipoles interacting with an external electric field. Its behaviour has been investigated by computer simulation in the limit of weak chirality. Large-scale (tertiary) helical winding induced along the field direction has been found above a threshold field E_c, and the helix parameters have been calculated as functions of the field strength. Below E_c there is no coherent helical structure of the chain conformation. We find a characteristic scaling of the threshold and the winding radius a with the chain bending modulus ε, $(E_c/k_{\rm B}T) \sim \varepsilon^{1/4}$ and $a \sim (k_{\rm B}T/E)\varepsilon$.

PACS. 61.20.Ja Computer simulation of liquid structure – 36.20.-r Macromolecules and polymer molecules – 87.15.By Structure, bonding, conformation, configuration, and isomerism of biomolecules

1 Introduction

Notwithstanding the very large configuration space available to them, many biopolymers, such as polypeptides and proteins, often adopt unique conformations [1]. Of particular interest amongst these are secondary helical structures, of which DNA is perhaps the best-known example. Helical geometry is a consequence of the interplay of hydrogen bonds forming between different groups within the molecule, and the sterical constraints which the same must satisfy. Upon variation of some external parameter such as temperature, solvent composition, or pH, a conformational transformation can be induced where an ordered, rod-like helix transforms into a random coil; this is the so-called helix-coil 'transition', which can be detected, *e.g.*, by monitoring the optical rotation or the viscosity of the sample [1]. The classical theories thereof date from the 1960s (see [2] for a review); more recent efforts, including computer simulations, have concentrated on detailed calculations for particular molecules (see, *e.g.*, [3,4] and references therein).

The natural question to ask at this stage is, what is the minimal model of a helix? Unsurprisingly, most theoretical work on helical polymers has been concerned with DNA. In 'supercoiled' DNA, occurring in bacteria, circular (*i.e.*, closed-loop) molecules arrange themselves into helices on a length scale (typically 50 nm) which is much larger than the double-helix repeat distance (3.4 nm) (for a review of supercoiling see [5]). Such 'tertiary structures' can be accounted for by treating DNA as a circular elastic rod [6]. Also in the semi-microscopic models [7,8] supercoiling is a consequence of twist rigidity, which presupposes a non-trivial (effectively ribbon-shaped) backbone. By contrast, in Marko and Siggia's more microscopic model [9, 10], chirality is introduced by imposing conservation of the linking number, *i.e.*, the number of times the two threads wind around each other. Elegant though this formulation might be, it is none the less restricted to ring molecules.

Here we present what is, to our knowledge, the first microscopic model of the tertiary structure of a chiral, helix-forming polymer in an external (electric) field. This paper is organised as follows: we start by writing down the Hamiltonian of a semi-flexible, chiral polymer chain with transverse dipoles along its backbone. We then proceed to eliminate the transverse variables and obtain an effective Hamiltonian which is a function of the unit tangent vector only, but contains an effective chiral coupling to the external field. Simulation results are then presented for the effect of the external field upon chain conformations. We find a non-monotonic behaviour in the chain correlations, indicating a coherent large-scale helical winding around the direction of the field. This ordering occurs above a threshold value of the field, below which no consistent direction of the helix has been observed; the threshold electric field exhibits a clear scaling dependence on the chain bending modulus. We conclude with a summary and a discussion of future directions.

2 Theory

Several theoretical models and approaches have been developed to treat chiral, and especially helically twisted, polymers; these originate mainly in the physical chemistry of biopolymers. Here we shall use the basic and explicitly tractable formalism of a semi-flexible polymer chain [11], in which chirality is introduced by means of a specific interaction between neighbouring segments. Strictly

[a] e-mail: emt1000@cus.cam.ac.uk

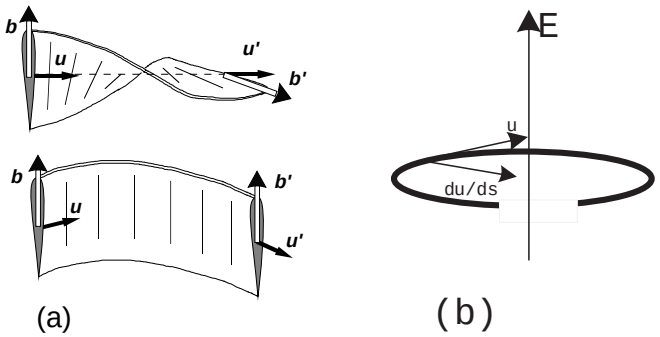

Fig. 1. (a) A chiral polymer chain with asymmetric cross-section is characterised by its secondary helical structure, with the transverse vector $\hat{\mathbf{b}}(s)$ twisting about the tangent $\hat{\mathbf{u}}$; this is the coupling of strength γ_t in equation (1). Untwisting the helix leads to bending of the chain due to the steric dipole in its cross-section (and so the corresponding constant γ_b should be proportional to the degree of asymmetry of this cross-section). Here the primes do *not* denote differentiation. (b) A continuous, coarse-grained worm-like chain described by equation (2). The effective chiral coupling induces local winding around $\mathbf{E}$.

speaking, even a simple curve represented by a coordinate $\mathbf{r}(s)$ (s is the arc length along the trajectory) can have chiral character: one can add to the standard bend elasticity $\frac{1}{2}\varepsilon\left(\frac{d\hat{\mathbf{u}}}{ds}\right)^2$, where $\hat{\mathbf{u}} = d\mathbf{r}/ds$ is the unit tangent vector, a spontaneous torsion term $\sim \left(\hat{\mathbf{u}} \times \frac{d\hat{\mathbf{u}}}{ds}\right) \cdot \frac{d^2\hat{\mathbf{u}}}{ds^2}$. Note that the apparent oddness of this coupling (or, in fact, any other similar chiral term) with respect to the transformation $\hat{\mathbf{u}} \to -\hat{\mathbf{u}}$, is of no consequence because such a change must be accompanied by a corresponding re-numbering of the monomer sequence, $s \to -s$, which makes the term invariant. However, a more natural description of a chiral polymer chain is *via* an additional variable – a transverse unit vector $\hat{\mathbf{b}}(s) \perp \hat{\mathbf{u}}(s)$ which can twist around, while moving along the chain backbone. Indeed, it has been argued that molecular biaxiality is essential to produce chirality in small-molecule fluids [12].

Figure 1a shows a spontaneously twisted chain modelled by an elastic 'belt' of asymmetric (sterically dipolar) cross-section. When two transverse vectors, $\hat{\mathbf{b}}(s)$ and $\hat{\mathbf{b}}(s')$, are forced to be parallel (for instance, by an external field), the chain will bend, preserving the sense of its natural chirality. These effects are expressed algebraically by the last two chiral coupling terms in equation (1) below. One may regard both the twist (γ_t) and the bend (γ_b) chiral coupling terms as extensions of the spontaneous torsion $\left(\hat{\mathbf{u}} \times \frac{d\hat{\mathbf{u}}}{ds}\right) \cdot \frac{d^2\hat{\mathbf{u}}}{ds^2}$: in both cases the role of the second-derivative field is taken by the corresponding perpendicular vector. Furthermore, one must take into account the torsion elasticity of such a chain, $\frac{1}{2}C\left(\frac{d\hat{\mathbf{b}}}{ds}\right)^2$. In some cases, *e.g.*, for elastic beams [13], the torsion modulus C can be related to the bending modulus ε: for a beam of rectangular cross-section with dimensions $h \ll d$, we have $\varepsilon = \frac{1}{12}Ydh^3$ and $C = \pi Ydh^3$, whence $C \simeq 12\pi\varepsilon$, where the Young modulus Y gives a characteristic energy scale. Yet no such relationship seems *a priori* appropriate to the minimal polymer chain defined in terms of its essential geometry, the unit tangent $\hat{\mathbf{u}}$ and the binormal $\hat{\mathbf{b}}$, so we regard the two moduli as independent. The chain Hamiltonian then takes the form:

$$\beta\mathcal{H} = \int_0^L ds \left\{ \frac{1}{2}\varepsilon(\hat{\mathbf{u}}')^2 + \frac{1}{2}C(\hat{\mathbf{b}}')^2 - \mu(\mathbf{E}\cdot\hat{\mathbf{b}}) + \gamma_t(\hat{\mathbf{u}}\times\hat{\mathbf{b}})\cdot\hat{\mathbf{b}}' + \gamma_b(\hat{\mathbf{u}}\times\hat{\mathbf{b}})\cdot\hat{\mathbf{u}}' \right\}, \quad (1)$$

where the prime denotes the s-derivative, $x' \equiv dx/ds$, $\beta = (k_BT)^{-1}$, and we have also included the coupling between the external electric field $\mathbf{E}$ and the transverse molecular dipole moment $\mathbf{m}_\perp = m\hat{\mathbf{b}}$. In making equation (1) dimensionless, we have introduced the dipole moment per unit length $\mu = m/(\xi k_BT)$, with ξ the characteristic size of a dipolar monomer unit. (It turns out that the longitudinal dipole does not contribute to the effects we are interested in and is, therefore, not included here. The only consequence of the γ_t term in our calculations is an irrelevant, and presumably small, renormalisation of the optimal value ψ^*, see the Appendix).

There is a simple relation between the constants that is determined by the spontaneous torsion of a chiral polymer chain. Even a straight chain with $\hat{\mathbf{u}} = (0,0,1)$ has a helically twisted ground state with $\hat{\mathbf{b}} \sim (\sin 2\pi s/\mathsf{p}, \cos 2\pi s/\mathsf{p}, 0)$, with p the natural pitch of the torsional rotation of $\hat{\mathbf{b}}$ along and about the chain backbone $\hat{\mathbf{u}}$: $\mathsf{p} \simeq 2\pi C/\gamma_t$. This helical rotation corresponds to the so-called secondary structure of chiral polymers [1]. In this sense we consider here a chain well above the helix-coil transition, when no particular tertiary structure is spontaneously established. γ_b should be much smaller than γ_t because it involves, apart from the chain chirality, the steric dipolar asymmetry of the polymer cross-section.

We now argue that the characteristic scales of variation of $\hat{\mathbf{u}}$ and $\hat{\mathbf{b}}$ are very different. It seems reasonable to assume that the transverse vector $\hat{\mathbf{b}}$ is a significantly 'faster' variable than $\hat{\mathbf{u}}$ for a semi-flexible chain; many chiral polymers, such as proteins and DNA, have a characteristic pitch of spontaneous torsion of the order of nanometers (secondary structure), whereas the persistence length of their tertiary structure is much greater. Indeed, Moroz and Nelson [14] have recently estimated $C = 120$ nm for DNA, much larger than the bending modulus ε. Integrating out the transverse variables $\mathbf{b}(s)$ (see the Appendix for details), one obtains the effective Hamiltonian, depending only on the chain tangent vector:

$$\beta\mathcal{H}_{eff} = -L\phi + \int_0^L ds \left[\frac{1}{2}\widetilde{\varepsilon}\,(\mathbf{u}')^2 + \phi\mathbf{u}^2 - \widetilde{g}(\mathbf{u}'\times\mathbf{u})\cdot\mathbf{E} \right], \quad (2)$$

with renormalised chain bending modulus $\widetilde{\varepsilon} = \varepsilon - \frac{4}{9}C\gamma_b^2$ and a new chiral coupling term with a prefactor $\widetilde{g} = \frac{4}{9}C\gamma_b\mu$. In equation (2) ϕ is a Lagrange multiplier that results from implementing the constraint that $\hat{\mathbf{u}}$ is a unit vector. Recently Pitard *et al.* [15] have considered transverse dipole moments on a freely-jointed chain with

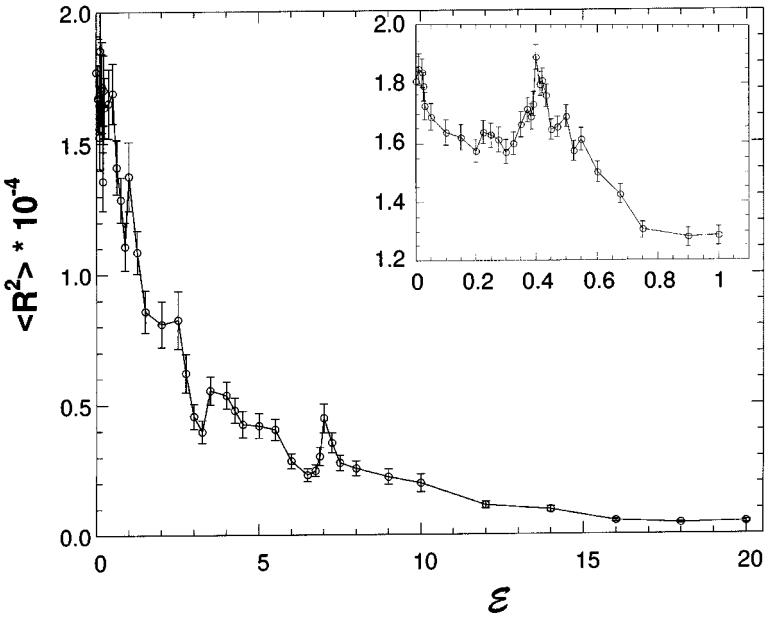

Fig. 2. Mean square of end-to-end distance as a function of the reduced field strength $\mathcal{E}$, for $\widetilde{\epsilon} = 10$ and averaged over $\mathcal{N} = 100$ chains of length $L = 1000$ (the line is drawn through the data points to guide the eye). The inset shows a more detailed investigation (the average of $\mathcal{N} = 1000$ chains to reduce errors) in the weak-field region. The chain size appears to be a non-monotonic function of the field.

excluded volume and chirality. The dipolar interactions were, however, treated within mean-field, and therefore only provide an attractive background to drive the collapse transitions, whereas chirality is only included in the last stage of writing down the Landau theory.

The secondary helical structure and helix-coil transition are determined by local chiral interactions on the nanometer scale, which do not involve an external field and depend on the microscopic details of the chain. In the present paper we concentrate on the effect of the field upon chain conformation on a larger length scale – the tertiary structure. It is noteworthy that the effective chiral term in equation (2) has a very similar functional form to the local torsion of a curve (see above). However, because it only couples the chain tangent and normal vectors in the plane perpendicular to **E**, there is no preference for upward or downward motion. Consequently, we expect this coupling to induce a helical winding along **E**, an externally defined direction in space (see Fig. 1b), with a radius determined by the balance against the elastic term, but with both senses of a helix equally represented.

3 Simulation

We have carried out off-lattice simulations of a single semi-flexible polymer chain in an electric field. As suggested by equations (1) and (2), in this first study we restrict ourselves to the phantom chain, neglecting the requirement of self-avoidance. The coupling between chain and field is as described in the preceding section. The semi-flexible chain has been modelled as a random walk in 3d space: the length of a step is taken as the unit of length and steps can be taken in any of a continuum of directions parametrised by the set of angles $\omega = (\theta, \phi)$, with probability (for $3 < i < L$)

$$P_i(\omega) = Z^{-1} \exp\left(-\beta\mathcal{H}_i\right), \qquad Z = \int d\omega \, \exp\left(-\beta\mathcal{H}_i\right) \quad (3)$$

$$\beta\mathcal{H}_i = -\widetilde{\epsilon}\hat{\mathbf{u}}_{i-1} \cdot \hat{\mathbf{u}}_i - \mathcal{E}(u^x_{i-1}u^y_i - u^y_{i-1}u^x_i), \quad (4)$$

where the unit vector $\hat{\mathbf{u}}_i = \mathbf{r}_i - \mathbf{r}_{i-1} = (u^x_i, u^y_i, u^z_i) = (\sin\theta\cos\phi, \sin\theta\sin\phi, \cos\theta)$. The discrete dimensionless Hamiltonian $\beta\mathcal{H}_i$ depends on two parameters: $\widetilde{\epsilon}$, the effective bending modulus in units of monomer length, $\xi = 1$; and $\mathcal{E} = \frac{4}{9}C\gamma_b m(E/\xi k_B T)$, the dimensionless ratio of the electric field **E** to the temperature, in the same units. We take **E** to be along the z-axis, $\mathbf{E} \equiv (0, 0, E)$. The first three steps in each random walk are unbiased (*i.e.*, all directions are equiprobable), which should be immaterial if the trajectory is sufficiently long. The angular integrations are performed by 24-point Gauss-Legendre quadrature [16]. Sampling is done by generating $\mathcal{N}$ chains of length $L \geq 1000$ each.

We start by investigating the behaviour of a chiral chain of fixed bending rigidity $\widetilde{\epsilon}$, as a function of the reduced field strength $\mathcal{E} \propto \beta E$; the dependence on $\widetilde{\epsilon}$ will be addressed later in the paper. In Figure 2 we present results for the mean squared end-to-end distance $\langle \mathbf{R}^2 \rangle$ of a chain of length $L = 1000$, as a function of the strength of the effective field, $\mathcal{E}$. Despite considerable statistical uncertainty, non-monotonic behaviour seems to be in evidence. Figure 3 shows snapshots of three 4000-segment chains for $\widetilde{\epsilon} = 100$ and increasing field strength $\mathcal{E} = 2$, 7 and 20. There is contraction of the chain dimensions along all three axes but it is more pronounced in the xy-plane,

Fig. 3. Snapshots of a single $L = 4000$ chain for $\widetilde{\epsilon} = 100$ and three increasing values of reduced field $\mathcal{E} = 2$, 7 and 20, from right to left. The field is along the z-axis and the threshold value for this chain is $\mathcal{E}_c \approx 7.5$. One can clearly see the marked reduction of chain dimensions in the xy-plane and the overall anisotropy of the dyration; the helical structure is more difficult to see because it occurs on a much smaller length scale.

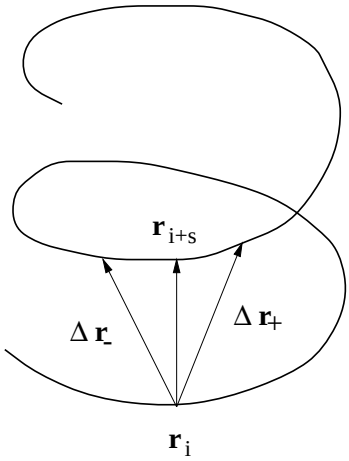

Fig. 4. Schematic representation of a portion of a helical molecule. $\Delta\mathbf{r}(s) = \mathbf{r}_{i+s} - \mathbf{r}_i$, which connects points separated by exactly one turn, is clearly shorter than either of the $\Delta\mathbf{r}_\pm$. Hence the order parameter τ^2 (basically an averaged squared length of $\Delta\mathbf{r}(s)$) should exhibit minima.

whence the apparent relative stretching along z. In addition, a large scale helical structure is clearly visible [17]. In order to quantify this, we start by noting that in a randomly coiled chain the mean squared distance between any two points increases linearly with their arc separation Δs (henceforth denoted s for simplicity). In a helix, by contrast, points separated by a single turn (or an integer number of turns) will be closer together than those that are slightly less, or slightly more than a full turn apart (see Fig. 4). In a statistical ensemble, the coherence of this effect will decrease as the number of turns increases, and eventually one recovers the ordinary diffusion law of the mean-square separation. Still, it should show up as the initial non-monotonic behaviour of the mean squared separation between any two points on the chain as a function of their separation s. There is a clear anisotropy in the correlation along the chain: due to the coupling symmetry we expect these correlations in the direction along $\mathbf{E}$ should not be significantly affected by the field, while the chain conformation in the plane perpendicular to $\mathbf{E}$ should reflect the induced winding. Thus motivated, we introduce a tensor order parameter

$$\tau^2_{\alpha\beta}(s) = \overline{\langle (r^\alpha_{i+s} - r^\alpha_i)(r^\beta_{i+s} - r^\beta_i)\rangle_{\{i\}}}. \qquad (5)$$

where the inner average is over all points i (monomers) of *one* chain ($i = 1, 2, \ldots, L$), and the outer average is over $\mathcal{N}$ different chains. Obviously the statistics will be much worse for $s \sim L$ (points far apart) than for $s \sim 1$ (points close together), since the latter corresponds to averaging many more pairs of points on a chain. However, as we shall see below, we are mostly interested in the region of small separations $s < 100$, so it suffices to take $L \gtrsim 1000$.

Because the external field (and hence the expected helix axis) is taken along z, it is convenient to write the order parameter in terms of its principal values, $\tau^2(s) = \tau^2_\perp(s) + \tau^2_z(s)$, with

$$\tau^2_\perp(s) = \overline{\langle (x_{i+s} - x_i)^2 + (y_{i+s} - y_i)^2\rangle_{\{i\}}}, \qquad (6)$$

$$\tau^2_z(s) = \overline{\langle (z_{i+s} - z_i)^2\rangle_{\{i\}}}. \qquad (7)$$

Recalling that the parametric representation of a helix is $x = a\cos(\chi s)$, $y = a\sin(\chi s)$, $z = bs$, with a the radius, b proportional to the pitch and χ a 'winding number', respectively, it is not difficult to check that for a perfect helical curve $\tau^2_z(s) \sim s^2$, whereas $\tau^2_\perp(s)$ will oscillate with a first minimum at $s^* \sim 2\pi/\chi$. Figure 5 illustrates the variation of $\tau^2_\perp$ with increasing arc separation s, calculated according to equation (6). The period (pitch) along

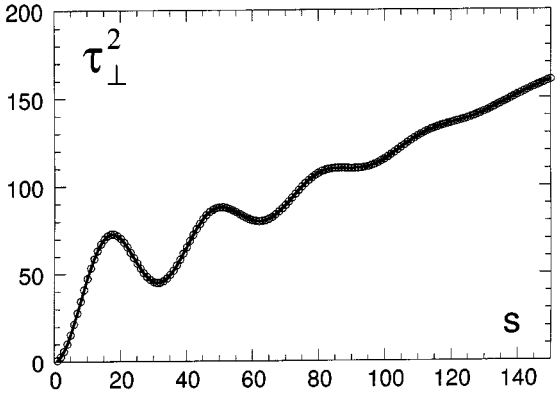

Fig. 5. $\tau^2_\perp$ *vs* s for $\widetilde{\epsilon} = 100$, $\mathcal{E} = 20$. Each point is obtained by averaging over 100 chains of length 4000. Although the standard deviations (not shown) are considerable, an oscillatory structure is clearly discernible. The second and higher minima tend to be diffused by increasing the number $\mathcal{N}$ of chains in the sample, whereas the first minimum remains, as far as we could ascertain, unaffected.

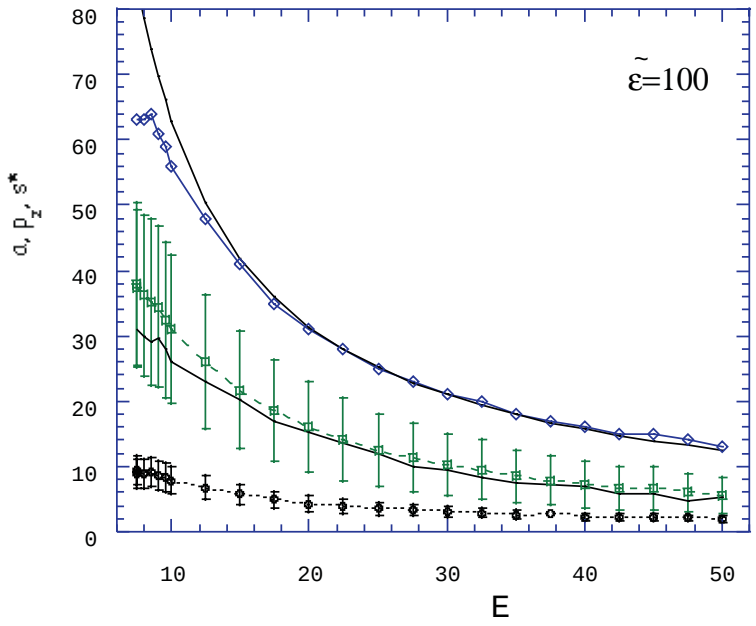

Fig. 6. Location of first minimum s^* (diamonds and solid line), the helix radius a (circles and dotted line), and the period along axis p_z (squares and dashed line), *vs* $\mathcal{E}$ for $\widetilde{\epsilon} = 100$ (averaged over 100 chains of length 4000). The error in s^* is estimated as ± 2 at worst, and the lines are drawn to guide the eye. Below $\mathcal{E} \sim 7.5$ no minimum of $\tau_\perp^2$ could be found. The lower solid line is the alternative route to p_z, equation (9).

the axis of an ideal helix is

$$\mathsf{p}_z = \frac{2\pi b}{\chi} = \frac{2\pi}{\chi}\sqrt{1 - a^2\chi^2}. \tag{8}$$

The position of the first minimum, s^*, for given values of $\widetilde{\epsilon}$ and $\mathcal{E}$ has been found by inspection of the curves $\tau_\perp^2$ *vs* s. As the axes of the helical sections of our trajectories are often slightly tilted relative to the $z-$axis, we approximate

$$\mathsf{p}_z \approx \sqrt{\tau^2(s = s^*)}, \tag{9}$$

as an alternative definition of pitch. Furthermore, the total arc length travelled along the chain in *one* turn of the helix is expressed *via* the Pythagoras construction, $(s^*)^2 \approx (2\pi a)^2 + \tau_z^2(s = s^*)$, where the first term on the right hand side is the (squared) circumference of the projection of the turn onto the xy-plane, and the second the (squared) displacement along z, whence

$$a \approx \frac{\sqrt{(s^*)^2 - \tau^2(s^*)}}{2\pi}\,. \tag{10}$$

Neglecting the uncertainty in the determination of s^* as comparatively small, the errors are given by standard statistical formulae as:

$$\Delta a = \frac{\Delta\tau_z^2(s^*)}{4\pi\sqrt{\tau_z^2(s^*)}}, \tag{11}$$

$$\Delta(\mathsf{p}_z) = \frac{\Delta\tau^2(s^*)}{2\sqrt{\tau^2(s^*)}} \tag{12}$$

and are probably overestimated because, in fact, the different pairs of points along the same chain are not always statistically independent.

In Figure 6 we plot the induced supercoiling parameters s^*, the winding radius a (from Eq. (10)) and the pitch p_z (from Eq. (9)), as functions of the effective field strength $\mathcal{E}$, for $\widetilde{\epsilon} = 100$. Each point results from averaging 100 chains of length 4000; a few trial runs with $L = 10000$ showed no deviation in the position of the first minimum of $\tau_\perp^2(s)$. Most noteworthy is the fact that there exists a critical field $\mathcal{E}_c$ below which $\tau^2(s)$ is monotonic; examination of snapshots of chains below this threshold reveals that they still exhibit a vestigial helical structure, but it does not seem to be correlated over the length of the chain and is, therefore, not characterised by a well-defined length scale and order parameter. Above $\mathcal{E}_c$, all three quantities, s^*, a and p_z, are decreasing functions of (E/k_BT), corresponding to tightening of the helix. They appear to follow very closely a linear scaling relationship, for instance, the radius $a \sim \varepsilon/\mathcal{E}$, although the increasing length of computations prevented a more detailed investigation of the high field regime for $\mathcal{E} > 100$. As a check on the consistency of our procedure, we calculated p_z from equation (8), using a from equation (10) and $\chi = 2\pi/s^*$. This is shown as the thick solid line in Figure 6; agreement with p_z given by equation (9) (dashed line) is quite satisfactory.

In all the above calculations the effective chain bending modulus was taken to be $\widetilde{\epsilon} = 100$. We have repeated the same procedure for several different values to investigate the dependence of the twisting effect on chain rigidity. Two sets of winding parameters, for $\widetilde{\epsilon} = 50$ and $\widetilde{\epsilon} = 20$, are plotted in Figure 7 (where the errors are not marked, being similar to those in Fig. 6). As would be expected on physical grounds, decreasing the rigidity enables chains to bend on shorter length scales, following a linear scaling.

The one remarkable effect we find is the change in the threshold field $\mathcal{E}_c$ - stronger fields are required to order more rigid chains into helices. Plotting the threshold $\mathcal{E}_c$ against $\widetilde{\epsilon}$ we find a clear power-law scaling, shown in Figure 8: a least-squares fit yields $\mathcal{E}_c \sim \widetilde{\epsilon}^{\alpha}$ with $\alpha = 0.253 \pm 0.005$, close to (and not incompatible with, bearing in mind all sources of error) $\alpha = 1/4$. In fact, a fit

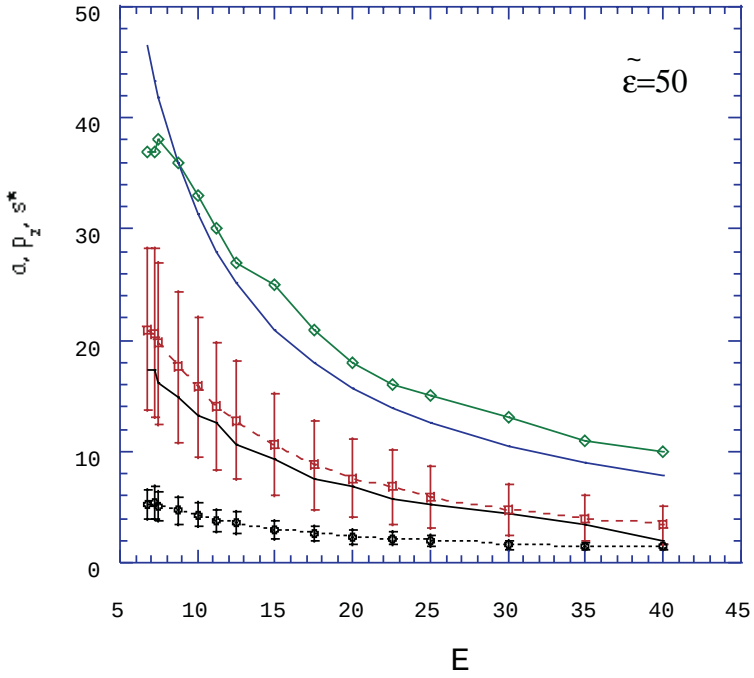

(a)

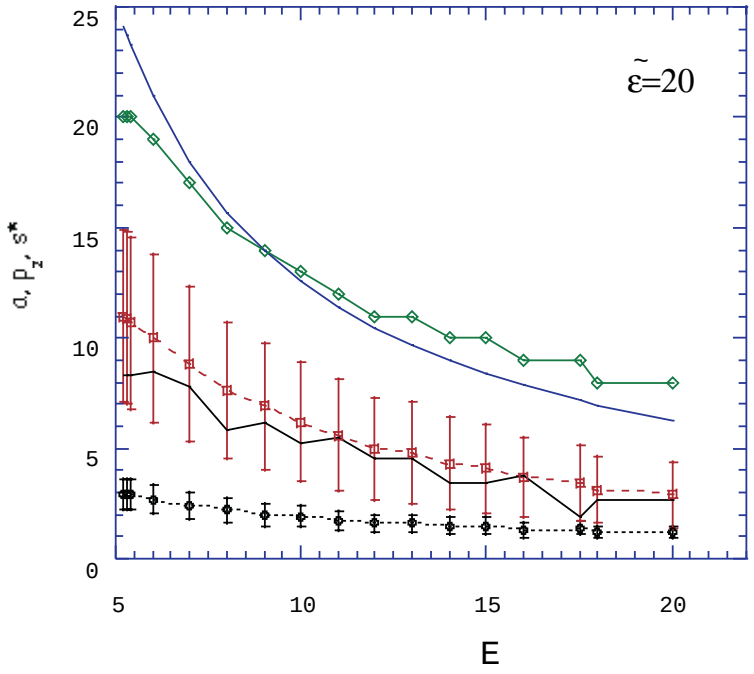

(b)

Fig. 7. Same as Figure 6, but for chains of different rigidity: (a) $\widetilde{\epsilon} = 50$; (b) $\widetilde{\epsilon} = 20$.

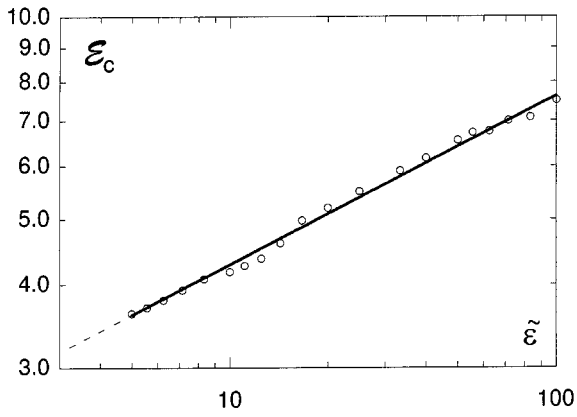

Fig. 8. Reduced threshold field $\mathcal{E}_c$ *vs.* bending rigidity $\widetilde{\epsilon}$ (log-log plot). All data points are from averages over 100 chains of length $L = 4000$. The least-squares fit to a power law, $\mathcal{E}_c = A\varepsilon^{\alpha}$, yields $\alpha = 0.253 \pm 0.005$ with correlation coefficient 0.997. The solid line is the model scaling function $\mathcal{E}_c \simeq 2.4\widetilde{\epsilon}^{1/4}$.

with fixed exponent $\frac{1}{4}$ (see Fig. 8) leads to the relation:

$$\frac{4}{9} C\gamma_b m \left(\frac{E_c}{\xi k_B T}\right) \simeq 2.409 \left(\frac{\widetilde{\varepsilon}}{\xi}\right)^{1/4} . \qquad (13)$$

Such a clear scaling behaviour requires a brief qualitative analysis. The winding around the direction of **E** is caused by the balance between the chain bending elasticity and the effective chiral coupling. By optimising the generic helical trajectory (an assumed minimum of energy) $\{x = a\cos(2\pi s/s^*);\ y = a\sin(2\pi s/s^*);\ z = bs\}$, one obtains the characteristic arc length periodicity $s^* \approx 2\pi(\varepsilon/\mathcal{E})$, as observed in Figures 6 and 7. Since the sense of helix is irrelevant for the chosen model, we may assume the simplest case of a flat circular trajectory of radius a, the energy density then takes the form of an effective potential: $\beta V(a) \sim \frac{1}{2}\varepsilon(1/a^2) - \mathcal{E}(1/a)$ per unit length of the chain, leading to the optimal winding radius $a^* \sim \varepsilon(k_BT/E)$, as in Figures 6 and 7. The local mean square fluctuation of this radius is $\langle|\Delta a|^2\rangle \sim 1/\left(L\,\partial^2 V/\partial a^2\right)_{a^*} \sim \varepsilon^3/\mathcal{E}^4 L$. An estimate for the transition point may be obtained by relating this fluctuation to the natural chain length scale, the persistence length $\sim \varepsilon$. This leads to $\mathcal{E}_c \sim (\varepsilon/L)^{1/4}$, not unlike the result in Figure 8.

4 Conclusions

In this preliminary simulation study of a chiral polymer chain coupled with an external field, we have neglected the spontaneous torsion of the chain, $\left(\hat{\mathbf{u}} \times \frac{d\hat{\mathbf{u}}}{ds}\right) \cdot \frac{d^2\hat{\mathbf{u}}}{ds^2}$, and concentrated instead on the large scale structure produced by the coarse-grained effective chiral coupling between the field and the transverse dipole moments of the monomers. As a result, the sense of induced helical winding was not retained in the resulting simulated conformations. However, the effect of the effective chiral coupling with the external field has been pronounced and found to exhibit a number of unexpected features, namely:

1. The overall chain size as measured by the squared end-to-end distance, varies non-monotonically with electric field strength.
2. Above a threshold field, at $\mathcal{E} > \mathcal{E}_c$, the chain conformation is a helix of well-defined pitch and radius, both of which are monotonically decreasing inverse functions of $\mathcal{E}$.
3. Below the threshold the chain still winds around the direction of the field, but the winding radius seems uncorrelated over the length of the chain. Such behaviour is reminiscent of the helix-coil transition (in zero field), separating regimes where the chain consists of one long, or a number of short, disconnected, helical sections, respectively.
4. Finally, the simulation produced, with a very high accuracy, a simple scaling dependence of the winding parameters, a^* and s^* and of the threshold field (E_c/k_BT) on the chain bending modulus ε.

The effect of lowering the chain rigidity is to make the chain more 'fractal' and thus able to bend on shorter length scales (*cf.* Figs. 3, 6 and 8). $\mathcal{E}_c$ is an increasing function of $\widetilde{\epsilon}$ characterised by an apparent 'critical exponent' $\alpha \simeq 1/4$, but the helical structure appears to survive unscathed in quite flexible chains, where no qualitatively different behaviour from that obtained for more rigid chains, $\widetilde{\epsilon} = 100$, is observed.

We are not aware of experiments that attempted inducing the helical winding by the application of an external electric field. However, it appears that the effect described here is within the plausible range of parameters and could be possible to observe. To illustrate this, we suggest the following estimate. Assume we are given a chiral polymer chain with transverse dipole moment on each monomer unit. The typical size of monomers can be around $\xi \sim 5$ Å and a moderate dipole strength is $m \sim 10^{-29}$ Cm. In a series of recent papers [8,14] the elastic moduli of a typical chiral protein or DNA molecule are given: bending constant $\varepsilon \sim 10$ nm, twist constant $C \sim 100$ nm and the natural pitch of secondary helical twisting $\mathsf{p} \sim 3$ nm. This makes the twist chiral coupling constant $\gamma_t \sim 10^{-7}$. Let us assume that the bend chiral coupling (which invloves an additional small factor, the steric dipole of the chain cross-section) is an order of magnitude smaller, $\gamma_b \sim 10^{-8}$. Now, substituting these parameters into equation (13) we obtain the threshold electric field required: $E_c \sim (\widetilde{\varepsilon}/\xi)^{1/4}(\xi k_BT/C\gamma_b m) \sim 4 \times 10^5$ V/m. This is not an exceptionally high field and, one might hope, the electrically-induced tertiary winding of chiral polymers will be experimentally observed.

We thank S. F. Edwards, M. Warner, Y. Mao, V. J. Anderson and T. A. Waigh for many stimulating discussions and suggestions. Financial support from the EPSRC is gratefully acknowledged.

Appendix: Integration of the transverse modes of a chiral polymer chain with transverse dipoles

This Appendix gives a more detailed treatment of the microscopic model of a polymer chain with chiral interactions in an external electric field. The corresponding partition function is expressed as a path integral over the tangent vector $\hat{\mathbf{u}}(s)$ and the transverse vector $\hat{\mathbf{b}}(s)$:

$$\mathcal{Z} = \int \mathcal{D}[\hat{\mathbf{u}}]\mathcal{D}[\hat{\mathbf{b}}] \prod_s \delta(\hat{\mathbf{u}}^2-1)\delta(\hat{\mathbf{b}}^2-1) e^{-\int ds\, \frac{1}{2}\varepsilon(\hat{\mathbf{u}}')^2} \times e^{-\int ds \left[\frac{1}{2}C(\hat{\mathbf{b}}')^2 - \mu(\mathbf{E}\cdot\hat{\mathbf{b}}) + \gamma_t(\hat{\mathbf{u}}\times\hat{\mathbf{b}})\cdot\hat{\mathbf{b}}' + \gamma_b(\hat{\mathbf{u}}\times\hat{\mathbf{b}})\cdot\hat{\mathbf{u}}'\right]}, \tag{A.1}$$

where the prime denotes differentiation with respect to s, ε is the bending modulus, and C is the torsion elasticity of the chain. The chiral coupling terms involving γ_t and γ_b are graphically represented in Figure 1b, and have been discussed in Section 2. μ is proportional to the transverse dipole moment of a monomer (in our model, the longitudinal dipole does not contribute to the induced chain twisting).

Although the Hamiltonian is only quadratic in the fields $\hat{\mathbf{u}}(s)$ and $\hat{\mathbf{b}}(s)$ (treated separately), the unit length constraint renders the problem of evaluating the partition function highly non-linear. One possible approach is to exponentiate the δ-functions in equation (A.1) by introducing auxiliary fields. In the steepest-descent (or mean-field) approximation (where the local constraints, $\hat{\mathbf{u}}^2 = 1$ and $\hat{\mathbf{b}}^2 = 1$, are relaxed into the global ones, $\langle\hat{\mathbf{u}}^2\rangle = 1$ and $\langle\hat{\mathbf{b}}^2\rangle = 1$), the partition function takes the form

$$\mathcal{Z}_{MF} = \int d\phi d\psi \mathcal{D}[\mathbf{u}]\mathcal{D}[\mathbf{b}]\, e^{i(\phi+\psi)L} e^{-\int ds \left[\frac{1}{2}\varepsilon(\mathbf{u}')^2 + i\phi\mathbf{u}^2\right]} \times e^{-\int ds \left[\frac{1}{2}C(\mathbf{b}')^2 - \mu(\mathbf{E}\cdot\mathbf{b}) + i\psi\mathbf{b}^2 + \gamma_t(\mathbf{u}\times\mathbf{b})\cdot\mathbf{b}' + \gamma_b(\mathbf{u}\times\mathbf{b})\cdot\mathbf{u}'\right]}. \tag{A.2}$$

It is convenient to incorporate the imaginary unit i into the definition of auxiliary fields ϕ and ψ. These fields can be treated as constants within the present approximation, and play the role of Lagrange multipliers in the effective free energy. Now that the unit-vector constraints have been removed, the elements of the path integral are ordinary 3-dimensional vectors $\mathbf{u}$ and $\mathbf{b}$, varying between $-\infty$ and $+\infty$, and therefore the integrals can be treated as Gaussian.

The next simplifying assumption we require is that the characteristic scales of variation of $\mathbf{u}$ and $\mathbf{b}$ be very different. This has been justified in Section 2, and is necessary in order to decouple the Fourier (Rouse) modes of $\mathbf{u}$ and $\mathbf{b}$ in the cubic chiral terms multiplying γ_t and γ_b, so that the fluctuations of $\mathbf{b}$ can be integrated as if on the background of a 'slowly-changing' $\mathbf{u}$. The procedure is now straightforward, since we have only Gaussian integrals in the 'fast' variable $\mathbf{b}$ in equation (A.2). However, care should be taken when dealing with the vector product chiral coupling term multiplying γ_t. Let us introduce a set of discrete Rouse modes (for a finite chain of length L):

$$\mathbf{b}(s) = \sum_{n=-\infty}^{+\infty} e^{2\pi i n(s/L)} \tilde{\mathbf{b}}_n;$$
$$\tilde{\mathbf{b}}_n = \frac{1}{L}\int ds\, e^{-2\pi i n(s/L)} \mathbf{b}(s). \tag{A.3}$$

Here $\tilde{\mathbf{b}}_n$ is, in general, a complex function, with real and imaginary parts: $\tilde{\mathbf{b}}_n \equiv \tilde{\mathbf{b}}_k = \Re[\tilde{\mathbf{b}}_k] + i\Im[\tilde{\mathbf{b}}_k]$; $\Im[\tilde{\mathbf{b}}_k] = -\Im[\tilde{\mathbf{b}}_{-k}]$, where $k = 2\pi n/L$. This distinction matters to the chiral coupling term in the Hamiltonian, the Fourier transform of which is

$$\int ds\, (\mathbf{u}\times\mathbf{b})\cdot\mathbf{b}' \Rightarrow 2L\sum_{n\geq 0} k\left\{\left(\mathbf{u}\times\Im[\tilde{\mathbf{b}}_k]\right)\cdot\Re[\tilde{\mathbf{b}}_k]\right\}, \tag{A.4}$$

where we have used the fact that $\mathbf{b}(s)$ is real. The path integral with respect to the 'fast' variable $\mathbf{b}$ can now be evaluated by integrating separately the real and imaginary parts of $\tilde{\mathbf{b}}_k$:

$$\int \prod_{n\geq 0} d^3\Re[\tilde{\mathbf{b}}_k] d^3\Im[\tilde{\mathbf{b}}_k]\, e^{\beta L[\mu\mathbf{E} + \gamma_b(\mathbf{u}\times\mathbf{u}')]\Re[\tilde{\mathbf{b}}_0]} \times \exp\left[-L\sum_{n\geq 0}\left\{\left(\frac{1}{2}Ck^2+\psi\right)\left(\Re[\tilde{\mathbf{b}}_k]^2 + \Im[\tilde{\mathbf{b}}_k]^2\right) - 2\gamma_t k \epsilon_{\alpha\beta\gamma} u_\alpha \Im[\tilde{\mathbf{b}}_k]_\beta \Re[\tilde{\mathbf{b}}_k]_\gamma\right\}\right]. \tag{A.5}$$

Gaussian integration yields the effective Hamiltonian for the longitudinal variables, determined exclusively by the $k = 0$ mode:

$$\beta\mathcal{H}_{eff} = -\phi L + \int ds\left\{\frac{1}{2}\varepsilon(\mathbf{u}')^2 + \phi\mathbf{u}^2 + \frac{1}{4\psi}\left[\mu\mathbf{E} - \gamma_b(\mathbf{u}\times\mathbf{u}')\right]^2\right\}. \tag{A.6}$$

The optimal value ψ^* of the Lagrange multiplier is found by maximising the partition function. We assume that the chiral effects represent but a small correction to the behaviour of the chain, and can therefore be neglected when estimating a first, saddle-point, approximation to ψ^*. Setting $\mu = \gamma_b = \gamma_t = 0$ in expression (A.5) and performing the integrations over $\Re[\tilde{\mathbf{b}}_k]$ and $\Im[\tilde{\mathbf{b}}_k]$, we get

$$\int \prod_{n\geq 0} d^3\Re[\tilde{\mathbf{b}}_k] d^3\Im[\tilde{\mathbf{b}}_k]\, e^{-L\sum_{n\geq 0}\left(\frac{1}{2}Ck^2+\psi\right)\left(\Re[\tilde{\mathbf{b}}_k]^2 + \Im[\tilde{\mathbf{b}}_k]^2\right)} \simeq e^{\psi L - 3\sum_{n\geq 0}\log\left(\frac{1}{2}Ck^2+\psi\right)} \equiv e^{-\Phi(\psi)}, \tag{A.7}$$

where Φ is the ψ-dependent part of $\beta\mathcal{H}_{eff}$. Converting the sum over k into an integral over n, this becomes

$$\Phi(\psi) = -\psi L + \frac{3L}{2\pi}\int_0^{+\infty} dk\, \log\left(\frac{1}{2}Ck^2 + \psi\right), \quad \text{(A.8)}$$

which upon minimisation yields $\psi^* \simeq \frac{9}{8C}$. Substituting ψ^* into equation (A.6) and expanding the last term, we obtain equation (2), with a renormalised bending modulus $\widetilde{\varepsilon}$ of the twisted semi-flexible chain. The most important result is the effective chiral coupling of the chain tangent vector $\hat{\mathbf{u}}$ to the external field, $-\mathbf{E}\cdot(\mathbf{u}'\times\mathbf{u})$ in equation (2). This favours bend in the plane perpendicular to $\mathbf{E}$, with direction determined by the sense of chirality (constant γ_b).

References

1. C.R. Cantor, P.R. Schimmel, *Biophysical Chemistry* (W. H. Freeman, New York, 1980), Part III, Chap. 20.
2. D. Poland, H.A. Scheraga, *Theory of Helix-Coil Transitions in Biopolymers* (Academic Press, New York, 1970).
3. W. Schneller, D.L. Weaver, Biopolymers **33**, 1519 (1993).
4. D. Poland, J. Chem. Phys. **105**, 1242 (1996).
5. N.R. Cozzarelli, T.C. Boles, J.White, in *DNA Topology and its Biological Effects*, edited by N.R. Cozzarelli, J.C. Wang (Cold Spring Harbor, NY, 1990), Chap. 4.
6. C.J. Benham, Biopolymers **22**, 2477 (1983).
7. J.F. Marko, E.D. Siggia, Macromolecules **27**, 891 (1994).
8. Kamien R.D., Lubensky T.C., Nelson P., O'Hern C.S., Europhys. Lett. **38**, 237 (1997).
9. J.F. Marko, E.D. Siggia, Science **265**, 506 (1994).
10. J.F. Marko, E.D. Siggia, Phys. Rev. E **52**, 2912 (1995).
11. M. Doi, S.F. Edwards, *The Theory of Polymer Dynamics* (Clarendon Press, Oxford, 1986).
12. A.B. Harris, R.D. Kamien, T.C. Lubensky, Phys. Rev. Lett. **78**, 1476 (1997); ibid. **78**, 2867 (1997).
13. L.D. Landau, E.M. Lifshitz, *Theory of Elasticity* (Pergamon, Oxford, 1986).
14. J.D. Moroz, P. Nelson, Proc. Natl. Acad. Sci. USA **94**, 14418 (1997).
15. E. Pitard, T. Garel, H. Orland, J. Phys. I France **7**, 1201 (1997).
16. W.H. Press, S.A. Teukolsky, W.T. Vetterling, B.P. Flannery, *Numerical Recipes: The Art of Scientific Computing*, (Cambridge University Press, Cambridge, 1992).
17. All chains start at the origin of coordinates.